Structure Effects in Angle-Resolved High-Order Above-Threshold Ionization of Molecules

H. Kang,[1,2] W. Quan,[1] Y. Wang,[1,2] Z. Lin,[1,2] M. Wu,[1,2] H. Liu,[1] X. Liu,[1,*] B. B. Wang,[3,†] H. J. Liu,[4] Y. Q. Gu,[4] X. Y. Jia,[5,6] J. Liu,[5,6] J. Chen,[5,6,‡] and Y. Cheng[7]

[1]*State Key Laboratory of Magnetic Resonance and Atomic and Molecular Physics, Wuhan Institute of Physics and Mathematics, Chinese Academy of Sciences, Wuhan 430071, China*

[2]*Graduate School of Chinese Academy of Sciences, Beijing 100080, China*

[3]*Laboratory of Optical Physics, Institute of Physics, Chinese Academy of Sciences, Beijing 100190, China*

[4]*Fusion Research Center, Chinese Academy of Engineering Physics, P. O. Box 919-18, Mianyang, Sichuan Province, China*

[5]*Center for Applied Physics and Technology, Peking University, Beijing 100084, China*

[6]*Institute of Applied Physics and Computational Mathematics, P. O. Box 8009, Beijing 100088, China*

[7]*State Key Laboratory of High Field Laser Physics, Shanghai Institute of Optics and Fine Mechanics, Chinese Academy of Sciences, P.O. Box 800-211, Shanghai 201800, China*

(Received 10 June 2009; published 19 May 2010)

We present energy-resolved angular distributions of photoelectrons generated in above-threshold ionization (ATI) of nonaligned diatomic molecules N_2 and O_2 in high-intensity short laser pulses, with emphasis on the most energetic part of the spectra. The angular distribution for photoelectrons with energy of $10U_p$ (U_p: ponderomotive energy), i.e., the plateau cutoff in ATI spectra, is found to be broader in O_2 than in N_2. Resorting to the analyses from both an *S*-matrix theory and an intuitive semiclassical model, we attribute the observation to the effect of the ground state molecular orbital structure on high-energy electron emission in strong-field molecular ionization.

DOI: 10.1103/PhysRevLett.104.203001 PACS numbers: 33.80.Rv, 33.80.Wz, 42.50.Hz

When an atom or molecule interacts with an optical field of peak intensity around 10^{14} W/cm^2, the outmost electron is first tunnel ionized, accelerated in the oscillating electric field of the laser, and may be driven back to its parent ion. This recolliding process, being the core ingredient of the rescattering scenario [1], has initiated many interesting laser-induced phenomena. Among them, imaging the dynamics of complex molecules with the help of the recolliding electron current, has attracted a lot of attention in the strong-field physics community [2]. Recently, it was reported that the outmost molecular orbital of the N_2 molecule can be extracted from the high-order harmonic generation spectra using the tomographic procedure [3]. Therein, structural information of the molecule may be extracted from the recombination process of the recolliding electron with its parent ion.

Alternatively, laser-induced electron diffraction for imaging molecules was proposed a decade ago [4] and different strategies have been thereafter suggested to extract the molecular structure from photoelectron spectra recorded with ultrashort intense laser pulses [5,6]. More recently, it was proposed that the backscattering high-energy photoelectrons may be most suitable for imaging molecules [7]. For atoms, it has been experimentally demonstrated that the ion-electron differential scattering cross section can be extracted from the angle-resolved spectrum of the rescattered electron [8]. A more elaborate experiment on aligned molecules has revealed the energy dependence of the differential cross sections based on a comprehensive analysis of the rescattering kinematics [9].

In this Letter, we present angle-resolved photoelectron energy spectra of nonaligned diatomic molecules N_2 and O_2, analyzing the effect of molecular orbital structure on high-energy photoelectron emission in strong-field molecular ionization. Note that the role of molecular orbital structure in ionization behavior of nonaligned molecules has been extensively addressed during the last decade. However, most studies were focused on the total ion yield [10] or the low-energy electron part [11]. Recent theoretical study has been performed on angular distribution (AD) of high-energy electrons for aligned molecules and distinct electron emission patterns have been revealed for N_2 and O_2 due to the different structure of their ground state molecular orbits [12]. On the other side, experiments have been attempted along this direction [13,14]; however, no clear evidence has been found to be related to the molecular orbital structure effect.

Our analysis here relies on the extraction and comparison of the AD for the most energetic electrons, i.e., those electrons with energy of $10U_p$, which resides in the plateau cutoff regime in photoelectron spectra. Our data show a broader AD for those electrons in O_2 than in N_2. Calculations from both *S*-matrix formalism based on strong-field approximation (SFA) and simple semiclassical model are able to reproduce the experimental observation and unveil the role of the molecular orbital structure in the high-energy electron emission.

In our experiments, a commercial 1 kHz femtosecond Ti:sapphire laser system (Legend L-USP, Coherent Inc.) is used. The system delivers pulses with energies up to 1 mJ,

pulse duration of 35 fs and a central wavelength of 800 nm. The homebuilt photoelectron spectrometer is based on the time-of-flight principle and has been described in detail previously [15]. The base pressure of the spectrometer is maintained below 10^{-8} mbar and the sample gases are fed into the interaction chamber through a leak valve. No attempt is made to align the molecules. Photo-ionized electrons are detected by microchannel plates and recorded by a multihit time-to-digital converter. In order to obtain the energy-resolved AD, the photoelectron energy spectra are recorded as a function of the angle between the spectrometer axis and the laser polarization direction, which is rotated using a computer-controlled achromatic half-wave plate.

In Figs. 1(a) and 1(b), the angle-resolved photoelectron energy spectra for N_2 and O_2 at laser intensity of 8×10^{13} W/cm^2 are presented. For comparison, we also show in Fig. 1(c) the spectrum for Xe, for which a pronounced side lobe appears at intermediate electron energies, in agreement with previous measurements [16,17]. Comparing the overall feature of the ADs in molecules with that in atomic Xe, it is clear that, for the electrons in a broader intermediate energy range (15 to 40 eV), the distributions in molecules are much broader. Similar finding has been reported recently by Cornaggia *et al.* [13] and was attributed to a larger differential elastic cross section for forward-rescattered electrons by the molecular potential. Our results further suggest that this may be a universal feature for simple molecules.

In the following we will focus on the AD for the electrons with energy of $10U_p$, i.e., the cutoff of the ATI plateau. In a classical picture, these electrons were initially ionized from the target near a phase of 17° after the field maximum, returning with an energy near $3.17U_p$ and backscattered upon the parent ion core with a final energy of $10U_p$. The results are shown in Fig. 2(a) for Xe, N_2, and O_2. It is found that for N_2 and Xe, their electron yields decrease monotonically with the increase of the emission angle with respect to the laser polarization direction. In contrast, for O_2, one sees that the electron yield hardly changes for small emission angles and only drops at larger emission angles. We note that while this broader AD at $10U_p$ for O_2 is slightly dependent on the exact energy chosen, the major features are not.

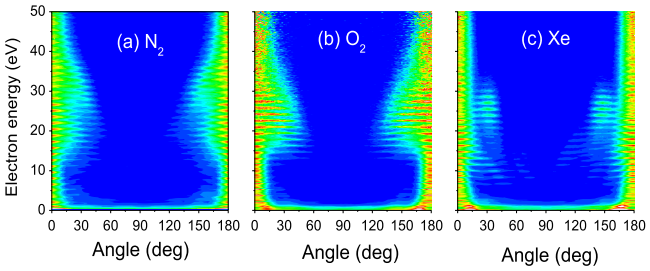

FIG. 1 (color online). Density plot of the angle-resolved photoelectron energy spectra of N_2 (a), O_2 (b), and Xe (c), respectively. The spectra are recorded with 35 fs, 800 nm laser pulses with peak intensity of 8×10^{13} W/cm^2.

Below we will show that this rather large high-energy back-rescattered electron emission probability at small angles off the laser polarization direction in O_2 can be ascribed to the effect of the molecular orbital structure on molecular ionization, based on the analysis from both an S-matrix theory and an intuitive semiclassical model.

The S-matrix formalism used here is an extension of the model previously employed in high-order ATI of atom [18], with the symmetry of the ground state molecular orbital incorporated. In brief, the differential ionization rate of a molecule in an intense laser field, within the framework of S-matrix theory, can be written as

$$\frac{dW}{d\Omega} = \int_0^\infty (2\pi)^{-3} p_f^2 dp_f 2\pi |T_{fi}|^2 \delta(E_f - E_i), \quad (1)$$

where $T_{fi} = T_d + T_r$, with T_d the direct and T_r the rescattering ATI transition matrix elements. Especially, the rescattering term T_r is

$$T_r = i\pi V_e^{-3/2} \sum_{k=0}^{k=\infty} \omega(u_p - j_0 - k) \langle p_f | U(r) | p_1 \rangle \psi(p_1) \times J_{q-j_0-k}(\zeta_1 - \zeta_f) \Im_{j_0+k}(\zeta_1, \eta), \quad (2)$$

where V_e is the normalization volume of the field, $u_p = U_p/\omega$, j_0 is the minimum photon number required by the electron to be ionized, q is the absorbed photon number for the transition between the initial and final state, $|p_1| = \sqrt{2\omega(j_0 + k - u_p - I_p/\omega)}$ and $|p_f| = \sqrt{2\omega(q - u_p - I_p/\omega)}$ where I_p is the ionization threshold. $J_{q-j_0-k}(\zeta_1 - \zeta_f)$ and $\Im_{j_0+k}(\zeta_1, \eta)$ are the Bessel and generalized Bessel functions, respectively, with $\zeta_{1(f)} = \sqrt{2u_p/\omega}\mathbf{p}_{1(f)} \cdot \hat{\epsilon}$ and $\eta = u_p/2$, $\hat{\epsilon}$ is the laser polarization direction. The function $\psi(p_1)$ is the molecular wave function in the momentum space [19] and $U(r)$ a two-center

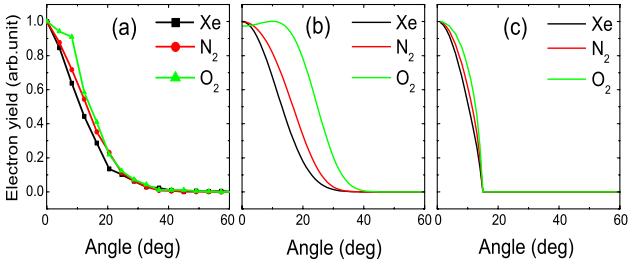

FIG. 2 (color online). (a) Experimental angular distribution for photoelectrons with kinetic energy of $10U_p$ (~48 eV) for Xe, N_2, and O_2. (b) Calculated angular distribution based on S-matrix formalism. (c) Calculated angular distribution with the semiclassical model. See the text for the details. The laser parameters are the same as in Fig. 1.

zero-range potential [20,21]. In Fig. 2(b), we present the AD of the ionized electron with energy of $10U_p$ for N_2, O_2 molecules and Xe atom, calculated with the above formalism. The results for molecules have been averaged over the random orientation of the internuclear axis. To compare directly with the data, all of the calculations have also been averaged over the spatial distribution of intensity within the laser focus. One can find that the AD for O_2 is wider than N_2 and Xe, which is qualitatively in agreement with the data shown in Fig. 2(a).

To gain further physical insight, we employ a simple semiclassical model to account for the different behavior in the AD for molecular N_2 and O_2 and demonstrate how the molecular structure affects the AD of most energetic electrons. In this model, an electron ensemble is subject to a laser pulse $E(t) = E_0 \sin\omega t$, where E_0 is the peak laser field amplitude and ω the laser angular frequency. The electrons reach the continuum via tunneling with a vanishing longitudinal velocity but nonzero transverse velocity. The initial tunneling times t_0 are uniformly distributed over one half optical cycle. In the atomic case, the electron ejection probability per unit time can be defined as $w(t_0, v_\perp) = w(t_0)w(v_\perp)$, where $w(t_0)$ is the tunneling rate [22] and $w(v_\perp)$ the transverse velocity distribution [23]. After tunnel ionization, the electrons will propagate under the influence of only the laser field. Some of them may return to the site of their release at $t_1 > t_0$, elastically scatter upon the ion core and further accelerate in the laser field, forming the ATI plateau. This model has been previously used to explain the main features observed in ATI of atoms, such as the $10U_p$ cutoff of high-energy plateau and the side lobes in the AD [24]. Here we extend this model to molecules.

In the molecular case, the dependence of the tunneling ionization on molecular alignment has to be considered and therefore the ionization probability for each electron trajectory may be written as $w(t_0, \theta, v_\perp) = w(t_0)w(\theta, v_\perp)$, where θ denotes the angle between the polarization axis of the ionizing field and the internuclear axis. Note that for this case, the quantum-mechanical transverse velocity distribution $w(\theta, v_\perp)$ is dependent on the alignment angle θ and closely related to the molecular orbital structure.

Within this model, the $10U_p$ part in the photoelectron spectrum comes from the electrons that tunnel at the phase of about 107° and backscatter by the core upon return with maximal kinetic energy of $3.17U_p$ at the phase of about 270°. In other directions than the laser electric field (the emission angle of the electron with respect to the field direction is still small), mainly two kinds of trajectories contribute to the $10U_p$ part: one corresponds to the electron that returns to the core with the maximal kinetic energy but scattered to other directions. Simple semiclassical calculation shows that the final energy E_k^f this electron can acquire from the field is less than $10U_p$. However, the energy gap of $(10U_p - E_k^f)$ may be compensated by its initial momentum perpendicular to the field direction when the electron tunnels out. The other one corresponds to the electron returning to the core with kinetic energy less than $3.17U_p$. No matter into which direction the electron will be scattered by the core, the final energy it can acquire is less than $10U_p$ and once again, the gap can be compensated by its initial perpendicular momentum. The $10U_p$ part in the spectrum therefore consists of those electrons emitted at various tunneling times and initial perpendicular momenta.

The calculated ADs of Xe, N_2, and O_2 for $10U_p$ electrons with this model are shown in Fig. 2(c). In general, the results reproduce well both experimental data and the S-matrix result, and especially the broader distribution of O_2 compared with that of Xe and N_2.

The difference of the ADs between O_2 and N_2 can be traced to the dependence of $w(\theta, v_\perp)$ on the ground state molecular orbital structure. In Fig. 3, we show the AD (corresponding to the initial perpendicular momentum distribution) of the tunneled electron for N_2 and O_2 at various alignment angles θ. The solid curves in Fig. 3 are calculated with the S-matrix theory [10], while the dashed curves correspond to the fitting of the solid ones obtained using appropriate $w(\theta, v_\perp)$ employed in the above semiclassical model to account for the molecular alignment influence on molecular ionization. From Fig. 3, one finds that, at different molecular alignment angles, the AD from O_2 is quite different from that in N_2, while the latter is very similar to atomic Xe (calculation not shown here) except at large alignment angles.

For example, when the molecular internuclear axis is aligned along the laser field, the ionization probability is maximal along the field direction for N_2. While for O_2, the maximal electron emission lies at an angle of ~30° off the laser field due to its antibonding π_g orbital. When the alignment angle increases, for O_2, the maximum of the AD tends to the field direction, coincides with it at around 30° and diverges from it again when the alignment angle is

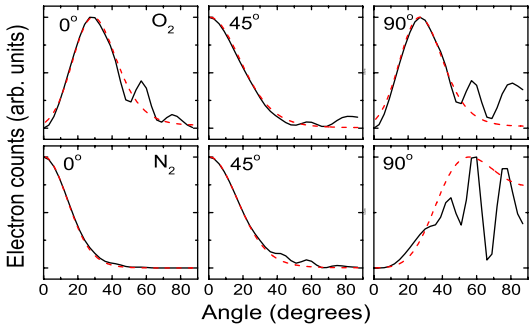

FIG. 3 (color online). Angular distribution of the tunneled electrons for O_2 (upper panel) and N_2 (lower panel) at various alignment angles θ. The black solid curves are obtained from S-matrix calculations, while the red dashed ones are obtained by using appropriate $w(\theta, v_\perp)$ to fit the quantum calculated curves. The laser parameters are the same as in Fig. 1.

larger than 45°, while for N_2, this maximum coincides with the field direction and only diverges from it at very large alignment angles close to 90°.

The broader AD of $10U_p$ electrons for O_2 compared with N_2 and atomic Xe can thus be understood as follows: as shown in Fig. 3, for most of the alignment angles in N_2, the AD of the tunneled electron decreases fast with angle. This corresponds to that the weight of the electron trajectory, $w(\theta, v_\perp)$ decreases fast with increasing perpendicular momentum. In contrast, for O_2, the AD increases with angle in a wide range of alignment angles, corresponding to that $w(\theta, v_\perp)$ increases with increasing $v_\perp$. Therefore, after averaging over the alignment angles, the emission probability of the $10U_p$ photoelectron decreases fast for N_2 but much more slowly for O_2 when the ejection angle increases, resulting in a broader AD in O_2 than N_2. The similarity between N_2 and Xe is due to the fact that, though the AD of N_2 at large alignment angles (see Fig. 3) is different from that of Xe, it has negligible influence on the high-energy photoelectron emission because the total ionization rate of N_2 at large alignment angle is far less than that at small alignment angles [19]. The marked difference in the $10U_p$ photoelectron angular distribution for O_2 and N_2 goes away for lower electron energies, because many other trajectories contribute, which return with different energies and scattered into different directions.

In conclusion, the energy-resolved ADs of photoelectrons from strong-field ATI of diatomic molecules are investigated and a broader AD for the most energetic ($10U_p$) electrons is found in O_2 than in N_2. Our analysis shows that this finding is closely related to the ground state molecular orbital structure, implying that angle-resolved high-order ATI spectra may be used for a detailed analysis of the properties of molecular systems.

We thank W. Becker for many useful discussions. This work is supported by NNSF of China (No. 10925420), the National Basic Research Program of China (No. 2006CB806000), and the CAEP Foundation (No. 2006z0202 and No. 2008B0102007).

Note added.—After submission of this Letter, a very similar work was published [25]. Therein, a suppression of electrons with intermediate energy of about $5U_p$ along laser field polarization for O_2 was found and ascribed to the destructive interference from various types of electron orbits with the help of an *S*-matrix treatment [12]. It should be noted that such a suppression is not observed in our data, pointing to the fact that this feature is rather sensitive to the laser parameters [14,25]. On the other side, in our calculation, minimums of the electron yield along the laser polarization for both O_2 and N_2 have been found at certain values of the laser intensity and the electron energy after averaging over the molecular orientation. However, after focal averaging, these minimums do not survive and only the comparatively broader AD of energetic electrons for O_2 is preserved as the main feature. Therefore it seems that the two-source double-slit interference as discussed in [25] is not relevant to our observation of the broader AD in O_2. More details will be given elsewhere [26]. Here we just mention that, theoretically, two different gauges (length gauge in [25] and velocity gauge in ours [20,21]) are adopted in the two works. Moreover, in our computation, the photoelectron emission probability for each alignment angle has been integrated over the azimuthal angles to consider three-dimensional distribution of the molecular orientation, in contrast to that a two-dimensional planar geometry is considered in the calculation of [25].

*xjliu@wipm.ac.cn
†wbb@aphy.iphy.ac.cn
‡chen_jing@iapcm.ac.cn

[1] P. B. Corkum, Phys. Rev. Lett. **71**, 1994 (1993).
[2] For a recent review, see, e.g., M. Lein, J. Phys. B **40**, R135 (2007).
[3] J. Itatani *et al.*, Nature (London) **432**, 867 (2004).
[4] T. Zuo *et al.*, Chem. Phys. Lett. **259**, 313 (1996).
[5] M. Spanner *et al.*, J. Phys. B **37**, L243 (2004).
[6] S. N. Yurchenko *et al.*, Phys. Rev. Lett. **93**, 223003 (2004).
[7] T. Morishita *et al.*, Phys. Rev. Lett. **100**, 013903 (2008); New J. Phys. **10**, 025011 (2008).
[8] M. Okunishi *et al.*, Phys. Rev. Lett. **100**, 143001 (2008); D. Ray *et al.*, *ibid.* **100**, 143002 (2008).
[9] M. Meckel *et al.*, Science **320**, 1478 (2008).
[10] See, for example, J. Muth-Böhm, A. Becker, and F. H. M. Faisal, Phys. Rev. Lett. **85**, 2280 (2000), and references therein.
[11] F. Grasbon *et al.*, Phys. Rev. A **63**, 041402(R) (2001).
[12] M. Busuladžić *et al.*, Phys. Rev. Lett. **100**, 203003 (2008).
[13] C. Cornaggia, Phys. Rev. A **78**, 041401(R) (2008).
[14] M. Okunishi *et al.*, J. Phys. B **41**, 201004 (2008).
[15] W. Quan *et al.*, Phys. Rev. Lett. **103**, 093001 (2009).
[16] B. Yang *et al.*, Phys. Rev. Lett. **71**, 3770 (1993).
[17] G. G. Paulus *et al.*, Europhys. Lett. **27**, 267 (1994).
[18] B. Wang *et al.*, Phys. Rev. A **75**, 063419 (2007).
[19] X. Y. Jia *et al.*, Phys. Rev. A **77**, 063407 (2008).
[20] Y. Guo, P. Fu, and B. Wang, Chin. Phys. Lett. **26**, 034204 (2009).
[21] Y. Guo *et al.*, Phys. Rev. A **80**, 063408 (2009).
[22] L. V. Keldysh, Sov. Phys. JETP **20**, 1307 (1965).
[23] N. B. Delone and V. P. Krainov, J. Opt. Soc. Am. B **8**, 1207 (1991).
[24] G. G. Paulus *et al.*, J. Phys. B **27**, L703 (1994).
[25] M. Okunishi *et al.*, Phys. Rev. Lett. **103**, 043001 (2009).
[26] B. Wang *et al.* (unpublished).